

# A Bag-of-Prototypes Representation for Dataset-Level Applications

Weijie Tu<sup>1</sup> Weijian Deng<sup>1</sup> Tom Gedeon<sup>2</sup> Liang Zheng<sup>1</sup>  
<sup>1</sup>Australian National University <sup>2</sup>Curtin University

## Abstract

*This work investigates dataset vectorization for two dataset-level tasks: assessing training set suitability and test set difficulty. The former measures how suitable a training set is for a target domain, while the latter studies how challenging a test set is for a learned model. Central to the two tasks is measuring the underlying relationship between datasets. This needs a desirable dataset vectorization scheme, which should preserve as much discriminative dataset information as possible so that the distance between the resulting dataset vectors can reflect dataset-to-dataset similarity. To this end, we propose a bag-of-prototypes (BoP) dataset representation that extends the image-level bag consisting of patch descriptors to dataset-level bag consisting of semantic prototypes. Specifically, we develop a codebook consisting of  $K$  prototypes clustered from a reference dataset. Given a dataset to be encoded, we quantize each of its image features to a certain prototype in the codebook and obtain a  $K$ -dimensional histogram. Without assuming access to dataset labels, the BoP representation provides a rich characterization of the dataset semantic distribution. Furthermore, BoP representations cooperate well with Jensen-Shannon divergence for measuring dataset-to-dataset similarity. Although very simple, BoP consistently shows its advantage over existing representations on a series of benchmarks for two dataset-level tasks.*

## 1. Introduction

Datasets are fundamental in machine learning research, forming the basis of model training and testing [18, 51, 52, 61]. While large-scale datasets bring opportunities in algorithm design, there lack proper tools to analyze and make the best use of them [6, 51, 56]. Therefore, as opposed to traditional algorithm-centric research where improving models is of primary interest, the community has seen a growing interest in understanding and analyzing the data used for developing models [51, 56]. Recent examples of such goal include data synthesis [29], data sculpting [25, 51], and data valuation [6, 32, 56]. These tasks typically focus on individual sample of a dataset. In this work, we aim to understand

nature of datasets from a dataset-level perspective.

This work considers two dataset-level tasks: suitability in training and difficulty in testing. **First**, training set suitability denotes whether a training set is suitable for training models for a target dataset. In real-world applications, we are often provided with multiple training sets from various data distributions (e.g., universities and hospitals). Due to distribution shift, their trained models have different performance on the target dataset. Then, it is of high practical value to select the most suitable training set for the target dataset. **Second**, test set difficulty means how challenging a test set is for a learned model. In practice, test sets are usually unlabeled and often come from different distributions than that of the training set. Measuring the test set difficulty for a learned model helps us understand the model reliability, thereby ensuring safe model deployment.

The core of the two dataset-level tasks is to measure the relationship between datasets. For example, a training set is more suitable for learning a model if it is more similar to the target dataset. To this end, we propose a vectorization scheme to represent a dataset. Then, the relationship between a pair of datasets can be simply reflected by the distance between their representations. Yet, it is challenging to encode a dataset as a representative vector, because (i) a dataset has a different cardinality (number of images) and (ii) each image has its own semantic content (e.g., category). It is thus critical to find an effective way to aggregate all image features to uncover dataset semantic distributions.

In the literature, some researchers use the first few moments of distributions such as feature mean and co-variance to represent datasets [20, 62, 74, 75, 82]. While being computational friendly, these methods do not offer sufficiently strong descriptive ability of a dataset, such as class distributions, and thus have limited effectiveness in assessing attributes related to semantics. There are also some methods learn *task-specific* dataset representations [1, 63]. For example, given a dataset with labels and a task loss function, Task2Vec [1] computes an embedding based on estimates of the Fisher information matrix associated with a probe network’s parameters. While these task-specific representations are able to predict task similarities, they are not suitable for characterizing dataset properties of interest. They

require training a network on the specific task [1] or on multiple datasets [63], so they are not effective in assessing the training set suitability. Additionally, they require image labels for the specific task, so they cannot be used to measure the difficulty of unlabeled test sets.

In this work, we propose a simple and effective bag-of-prototypes (BoP) dataset representation. Its computation starts with partitioning the image feature space into semantic regions through clustering, where the region centers, or prototypes, form a codebook. Given a new dataset, we quantize its features to their corresponding prototypes and compute an assignment histogram, which, after normalization, gives the BoP representation. The dimensionality of BoP equals the codebook size, which is usually a few hundred and is considered memory-efficient. Meanwhile, the histogram computed on the prototypes is descriptive of the dataset semantic distribution.

Apart from being low dimensional and semantically rich, BoP has a few other advantages. **First**, while recent works in task-specific dataset representation usually require full image annotations and additional learning procedure [1, 63], the computation of BoP does not rely on any. It is relatively efficient and allows for unsupervised assessment of dataset attributes. **Second**, BoP supports dataset-to-dataset similarity measurement through Jensen-Shannon divergence. We show in our experiment that this similarity is superior to commonly used metrics such as Fréchet distance [27] and maximum mean discrepancy [33] in two dataset-level tasks.

## 2. Related Work

**Dataset representations.** A common practice is to use simple and generic statistics as dataset representations [20, 62, 74, 75, 82]. For example, Peng *et al.* [62] use the first moment to represent a dataset. Deng *et al.* [20] use global feature mean and co-variance as dataset representations. Vanschoren *et al.* [82] find dataset cardinality (the number of images/classes) useful to encode a dataset. These methods have limited descriptive ability, whereas BoP is more semantically descriptive. Moreover, it is feasible to learn a *task-specific* dataset representation [1, 63, 85, 88]. For example, Ying *et al.* [85] learn transfer skills from previous transfer learning experiences for future target tasks. Achille *et al.* [1] propose to learn a task embedding based on the estimate of Fisher information matrix associated with a task loss. Compared with these task-specific representations, BoP is hand-crafted, avoiding computation overheads incurred by end-to-end learning. It is thus efficient in measuring training set suitability without training any models. Moreover, BoP require no image labels, making it more suitable for assessing the difficulty of unlabeled test sets.

**Dataset-to-dataset similarity.** We briefly review three strategies. **First**, some dataset similarity measures are developed in the context of domain adaptation [2, 9, 10, 86].

They typically depend on a loss function and hypothesis class, and use a supremum of that function class to quantify the similarity of datasets. (*e.g.*,  $\mathcal{H}\Delta\mathcal{H}$ -divergence [9],  $f$ -divergence [2], and  $\mathcal{A}$ -distance [10]). **Second**, dataset distance can be computed based on optimal transport [5, 17, 79]. For example, the squared Wasserstein metric Fréchet distance [27] is widely used in comparing the distribution discrepancy of generated images with the distribution of real images [39]. To better leverage the geometric relationship between datasets, Alvarez *et al.* [5] use labels to guide optimal transport towards class-coherent matches. **Third**, existing dataset representations can be used to compute dataset distance [33, 62, 75, 81]. For example, maximum mean discrepancy (MMD) [33] computes the distance between mean elements of distributions on the probability space. Peng *et al.* [62] eliminate dataset discrepancy by matching datasets moments. CORAL [75] uses the second-order statistics of datasets to measure distance. This work is in the third category and uses JS divergence between BoP representations to calculate dataset-to-dataset similarity.

**Assessment of training dataset suitability.** Recent works have focused on understanding the importance of *individual training instances* in training of neural networks [6, 32, 45, 56]. For example, Data Shapley [32] and Consistency Score [45] are proposed to evaluate the value of each data instance. Some methods identify “difficult” instances based on the information of training dynamics [7, 76, 80].

Different from the above approaches, this work studies the suitability of an *entire* training set. Given multiple training datasets from different data distributions, the focus is to choose the most appropriate training dataset for the target domain. Dataset-to-dataset similarity can be used for this goal. Intuitively, if a training dataset has high similarity with a target dataset, the model trained on it is expected to be more performant and vice versa. In this work, we use BoP representation coupled with simple JS divergence to calculate dataset-to-dataset similarity and demonstrate its effectiveness in accessing training set suitability.

**Assessing test set difficulty without ground truths.** The goal of this task (also known as unsupervised accuracy estimation) is to predict the accuracy of a given model on various unlabeled test sets. Existing methods usually use a representation of the test set for accuracy prediction [13, 19, 20, 30, 34]. Normally this representation is derived from classifier outputs, such as image features [20], prediction logits [30], average softmax scores [34]. Then, regression is used to establish the relationship between this representation and model test accuracy under various testing environments. Compared with existing dataset features, the BoP representation better characterizes the semantic distribution of training and test sets and thus can be effectively used for model accuracy prediction.

### 3. Methodology

#### 3.1. Bag-of-Words Model Across Communities

In **natural language processing** (NLP) and information retrieval, the Bag-of-Words (BoW) model [46, 47, 50, 57] vectorizes textual data as a word histogram. Specifically, for each word in the dictionary, its occurrences in a document are counted, which fills in the corresponding entry of the BoW feature. This word frequency vector is thus used to represent a document. Numerous improvements of the BoW feature were made in NLP, such as n-grams [47, 50] and term frequency-inverse document frequency [68].

In the early 2000s, the BoW representation was introduced to the **computer vision** (CV) community to encode hundreds or thousands of local image descriptors [8, 53] into a compact vector [73]. As there is no semantic codebook like in NLP, a visual codebook is constructed by performing clustering (*e.g.*, k-means) on a collection of local image features, where the resulting clustering centers are called “visual words”. Local image descriptors are quantized to their nearest cluster center so that a visual word histogram can be computed. This BoW histogram also have undergone extensive improvements in later years, such as Fisher vector [64, 65], vector of locally aggregated descriptors (VLAD) [43], and the use of principal component analysis and whitening [42].

**Contribution statement.** This paper contributes a baseline method in adopting the BoW idea study the two basic properties of a dataset. To this end, we propose to represent a dataset using its histogram over a series of prototypes. A comparison between the usage of BoW model in NLP, CV and our dataset-level research is shown in Table 1. Specifically, the BoP representation relies on clustering for codebook formation, has a relatively small codebook (depending on the richness of dataset semantics), and has semantically sensible codewords.

#### 3.2. Bag-of-Prototypes Dataset Representation

Given a dataset  $\mathcal{D} = \{\mathbf{x}_i\}_{i=1}^N$  where  $N$  is the number of images and a feature extractor  $\mathbf{F}(\cdot)$  that maps an input image into a  $d$ -dimensional feature  $f \in \mathbb{R}^d$ , we extract a set of image features  $\mathcal{F} := \{\mathbf{F}(\mathbf{x}_i)\}_{i=1}^N$ . While it is possible to directly use the dataset images (or features) as model input under small  $N$ , it becomes prohibitively expensive when  $N$  is large. We therefore focus on extracting useful semantic features of  $\mathcal{F}$  by encoding its image features into a compact representation. Below we detail the necessary steps for computing the proposed BoP representation (refer Fig. 1).

**Step I: Codebook generation.** Given a reference dataset  $\mathcal{D}_r = \{\mathbf{x}_i^r\}_{i=1}^{N_r}$ , we extract all of its image features  $\mathcal{F}_r := \{\mathbf{F}(\mathbf{x}_i^r)\}_{i=1}^{N_r}$  using a pretrained network, from which a codebook is constructed. Specifically, we adopt standard k-means clustering [54] to partition the feature space  $\mathbb{R}^d$

	BoW in NLP	BoW in CV	BoP
Encoded objects	Documents	Images	Datasets (a set of images)
Codewords in codebook	Words	Cluster centers of local descriptors	Prototypes of image features
Clustering?	No	Yes	Yes
Codewords semantics	Clear	Little	Sensible
Codebook size	$> 10^3$	$10^3 - 10^6$	$\sim 10^2$ (dataset dependent)

Table 1. Comparing BoP with BoW model in natural language processing (NLP) and computer vision (CV). The objective of BoW in NLP and CV is encoding texts and images respectively, while BoP is proposed to represent datasets.

into  $K$  clusters. Each of the  $K$  cluster centers is called a “prototype”, because oftentimes each center mainly represents a certain semantic content. See Fig. 1 right for exemplar image of each prototype. The prototypes, or centers, constitute the codebook, denoted as  $\mathcal{C} = \{\mathbf{c}_i\}_{i=1}^K$ , where  $\mathbf{c}_i$  is the  $i$ -th prototype. Note that, the order of the prototypes is fixed in the codebook.

**Step II: Histogram computation.** For a dataset to be encoded  $\mathcal{D}_e = \{\mathbf{x}_i^e\}_{i=1}^{N_e}$  where  $N_e$  is the number of images, we project it onto codebook  $\mathcal{C}$  of size  $K$  to compute its BoP representation. Specifically, after extracting image features  $\mathcal{F}_e := \{\mathbf{F}(\mathbf{x}_i^e)\}_{i=1}^{N_e}$  from  $\mathcal{D}_e$ , for each image feature, we compute its distance with all the  $K$  prototypes in the codebook, yielding  $K$  distances  $d_1, \dots, d_K$ , where  $d_i$  is the distance between an image feature and the  $i$ -th prototype. An image feature is quantized to prototype  $\mathbf{c}_i$  if  $d_i$  is the lowest among  $d_1, \dots, d_K$ . Following the quantization, we generate a  $K$ -dimensional one-hot encoding where the  $i$ -th entry is 1 and all the others are 0. Having computed the one-hot vectors for all the image features, we sum them which is then normalized by  $N_e$ , the number of images in  $\mathcal{D}_e$ . This gives the histogram representation  $\mathbf{h}_e$ , or **BoP representation**, for  $\mathcal{D}_e$  where the  $i$ -th entry indicates the density of features in  $\mathcal{D}_e$  belonging to prototype  $\mathbf{c}_i$ .

#### 3.3. Measuring Dataset-to-Dataset Similarity

Similar to image / document retrieval where BoW vectors of instances are used for similarity comparison [14, 26, 59, 66, 73], this work uses the BoP representation to calculate dataset-to-dataset similarity. Specifically, given BoP representations  $\mathbf{h}_x$  and  $\mathbf{h}_y$  of two datasets  $\mathcal{D}_x$  and  $\mathcal{D}_y$ , we simply define their similarity  $S_{x,y}$  using Jensen-Shannon divergence (JS divergence), which is designed for histogram-based similarity measurement [16, 55].

**Task-oriented similarity measure.** We can build a *universal* codebook on a large-scale dataset following BoW model [14, 87]. By doing so, the resulting BoP representations are generic. We can also build a *task-oriented* code-

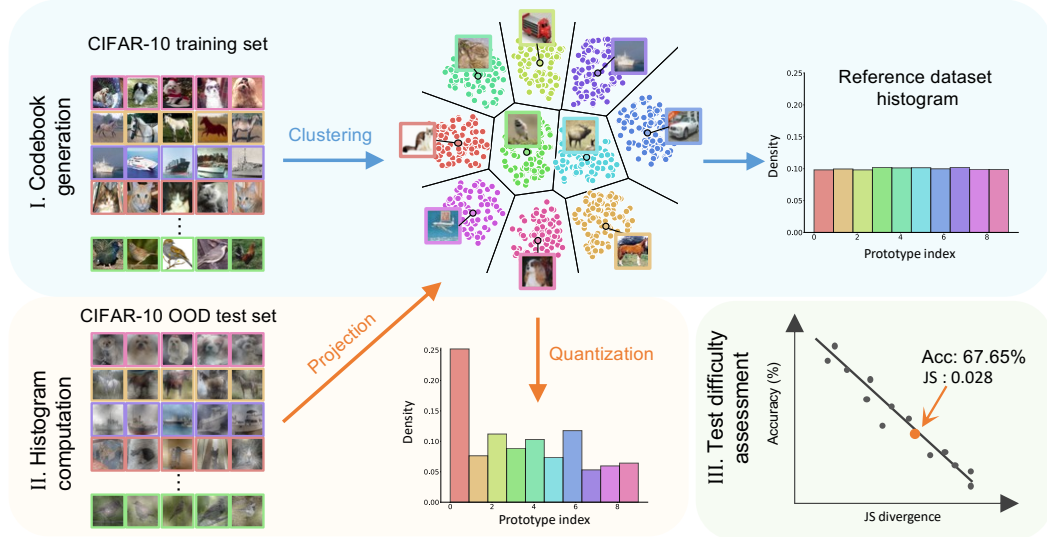


Figure 1. Workflow of BoP representation computation using CIFAR-10 [49] and one CIFAR-10 out-of-distribution (OOD) test set as an example. **Top:** We group image features of the reference dataset CIFAR-10 into 10 clusters, and the centers are called prototypes. The prototypes constitute the codebook of size 10. **Bottom left:** To encode the OOD test set, we project it onto the codebook by quantizing each image feature to its corresponding prototype. Lastly, we compute the histogram, *i.e.*, BoP representation, of CIFAR-10 OOD test set. **Bottom right:** We regard dataset-to-dataset similarity as the Jensen-Shannon divergence between BoP histograms of CIFAR-10 OOD test set and reference dataset. With such similarity, we can measure the test set difficulty for the model trained on reference dataset.

book on a reference dataset from a specific task to consider more task-oriented information. The latter is more suitable for the two dataset-level tasks considered in this work. For the task of training set suitability assessment, we use the target dataset as the reference for codebook generation to fully consider its semantic information. As a result, the JS divergence between BoP representations of the training set and the target dataset can well capture how a training set is similar to the target set. Similarly, for the task of test set difficulty assessment, we build codebook on the training set. This practice can effectively measure how an unlabeled test is similar to a given training set.

### 3.4. Discussion

**Working mechanism of BoP.** Codebook generation of BoP can be viewed as Centroidal Voronoi Tessellations [24]. Specifically, the prototypes (cluster centers) of codebook tessellate the feature space into Voronoi cells. Then, histogram computation approximates a probability distribution function in the same way as the *nonparametric* histogram [12, 28, 67]. That is, the BoP representation reflects the distribution of a dataset in the feature space.

As shown in Fig. 1, the prototypes of reference dataset tessellate feature space into Voronoi cells. Based on this, we quantify the histogram of the reference dataset to represent its distribution. Given a new dataset, we conduct the same histogram calculation procedure and correspondingly capture its dataset distribution with the histogram. Then, we measure discrepancy of the two datasets by calculating JS

divergence between their histograms. Compared with common measures of dataset distance (*e.g.*, FD [27], KID [11] and MMD [33]) that only reflect global structure (*e.g.*, first few moments) of dataset distributions, BoP, collaborated with JS divergence, considers more local structures.

#### Training set suitability vs. transferability estimation.

Two tasks relate but differ significantly: 1) Given an unlabeled target dataset and a pool of training datasets, the former aims to select the most suitable training set for the target. The latter assumes a labeled target dataset and a pool of models pretrained on a source dataset, with the goal of selecting the most suitable source model for the target without fine-tuning them all [3, 4, 60]; 2) Datasets in training set suitability are used for the same classification problem. In contrast, in transferability estimation, the problem in the target dataset (*e.g.*, CIFAR-10 classification) is different from that of the source dataset (*e.g.* ImageNet classification).

#### Analysis of the number of prototypes in a codebook.

The codebook size is a critical factor influencing the usefulness of the BoP. A small codebook means a coarser partition of feature space, where similar features will likely be in the same cluster, but dissimilar features may also be in the same cluster. Moreover, a large codebook provides a finer description of the space, where dissimilar features are quantized to different prototypes and more semantics are explored. According to our experiment results in Fig. 2 and Fig. 5, we find, reassuringly, BoP is robust against the codebook size: prototype number can deviate within a wide range around the true classes number (*e.g.*, 345 for Domain-



Net [62]) without significantly affecting performance.

**Application scope and future directions.** BoP is proposed to study the two dataset-level tasks, and the datasets considered in each task share the same label space. We may encounter some situations where we need to compare datasets with different label spaces (*e.g.*, pre-training datasets selection [1]). In this case, one potential way is to build a universal codebook on a large-scale and representative dataset similar to BoW models [14, 87]. By doing so, the resulting BoP representations can encode diverse and sufficient semantics for comparing datasets across various label spaces. We view our BoP as a starting point to encode datasets. It would be interesting to study other dataset vectorization schemes and dataset-level tasks.

## 4. Comparing Training Suitability of Datasets

This task studies dataset valuation where multiple training sets are provided by different data contributors. The goal is to select the most suitable training set (ideally without training) whose trained model performs the best on a target test set. In this section, we first validate that BoP, collaborated with JS divergence (BoP + JS), is predictive of dataset suitability for the target test set. Then, we show that BoP is robust when using a wide range of codebook sizes and different networks.

### 4.1. Experimental Settings

**Correlation study under DomainNet setup.** We use domain generalization benchmark DomainNet [62], which consists of 6 domains: Painting, Real, Infograph, Quickdraw, Sketch and ClipArt, where the tasks are 345-way object classification. Each domain has its training and test splits. We conduct the correlation study in an *leave-one-out* manner, leading to 6 groups of correlation studies, with each group using the test split of one domain as the target test set. Additionally, we apply image transformations to the training split of six original domains. Specifically, we employ ‘Cartoon’ [48], ‘Zoom Blur’ and ‘JPEG Compression’ [36] to convert domains’ style to be one specific type. We also use ‘AugMix’ [38] and ‘AutoAugment’ [15], which transform images with various operations to generate domains with mixed styles. This process synthesizes 30 new datasets, so we have 36 training sets in total.

We follow the training scheme provided by TLLib [44] to train ResNet-101 model [35], whose weights are pretrained on ImageNet [18], yielding 36 models. Moreover, penultimate outputs of pretrained ResNet-101 is used as image feature. On the test set, we generate a codebook of size 1000. Then, for each training set, we compute its BoP histogram, BoP + JS from the test set, and the accuracy of its trained model on the test set. After this, we calculate correlation strength between BoP + JS and model accuracy to evaluate whether BoP is indicative of datasets training suitability.

Method	ResNet-34			ResNet-101		
	$r$	$\rho$	$\tau_w$	$r$	$\rho$	$\tau_w$
FD [27]	-0.860	-0.926	-0.828	-0.903	-0.902	-0.802
MMD [33]	-0.817	-0.801	-0.691	-0.821	-0.817	-0.704
KID [11]	-0.773	-0.904	-0.804	-0.876	-0.896	-0.800
BoP + JS	<b>-0.960</b>	<b>-0.927</b>	<b>-0.840</b>	<b>-0.961</b>	<b>-0.929</b>	<b>-0.840</b>

Table 2. Compare averaged Pearson’s correlation ( $r$ ), Spearman’s correlation ( $\rho$ ) and weighted Kendall’s correlation ( $\tau_w$ ) of Fréchet distance (FD), maximum mean discrepancy (MMD), kernel inception distance (KID) and BoP + JS (codebook size 1000) on six test sets in DomainNet. We report two groups of results using ResNet-34 (Left) and ResNet-101 (Right). We show BoP + JS is more effective in assessing training set suitability than others.

**Evaluation metric.** We use Pearson’s correlation  $r$  and Spearman’s rank correlation  $\rho$  to show linearity and monotonicity between BoP-based dataset distance and model accuracy, respectively. Both metrics range in  $[-1, 1]$ . If  $|r|$  or  $|\rho|$  is close to 1, the linearity or monotonicity is strong, and vice versa. In addition to these two metrics, we also use weighted variant of Kendall’s correlation ( $\tau_w$ ) [83]. It is shown to be useful when selecting the best ranked item is of interest [71], while a major application of BoP + JS is to select the training dataset leading to the best performance on a test set. This metric has the same range where a number closer to  $-1$  or  $1$  indicates stronger negative or positive correlation, respectively, and  $0$  means no correlation.

### 4.2. Evaluation

**Strong correlation: A training set is more suitable for a given test set if it has small BoP + JS.** Fig. 2 shows correlation study on ClipArt, Painting, Real and Sketch. We notice that there are strong Pearson’s correlations ( $|r| > 0.95$ ), Spearman’s rank correlations ( $|\rho| > 0.93$ ) and relatively high weighted Kendall’s correlations ( $|\tau_w| > 0.84$ ) on four test sets. This suggests that BoP + JS is stable and useful across test sets. Table 2 compares average correlation strength of BoP + JS with Fréchet distance (FD) [27], maximum mean discrepancy (MMD) [33] and kernel inception distance (KID) [11]. They use that same image features as BoP. According to their formulae, mean and covariance of these features are used for distance computation. We see that BoP + JS has the highest average correlation scores on six test sets ( $|r| = 0.961$ ,  $|\rho| = 0.929$  and  $|\tau_w| = 0.840$ ). On average, BoP + JS is superior in depicting training sets suitability for a test set without any training procedure.

**Impact of codebook size** is shown in the Fig. 3. We construct codebooks with different size within approximately one order of magnitude around 345. We find that the three correlation scores increase and then become stable when codebook size becomes larger. This indicates that the per-

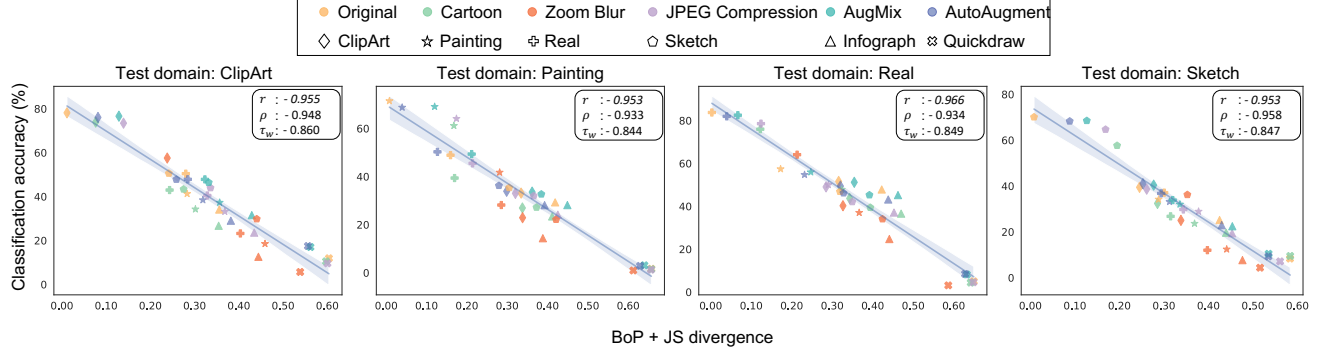


Figure 2. **Correlation study for training suitability of datasets.** We report the correlation strength between BoP + JS and model classification accuracy on four test domains of DomainNet: ClipArt, Painting, Real and Sketch. The model architecture is ResNet-101. Each dot denotes a model trained on a training set of DomainNet. We mark training domains (e.g., ClipArt) by different shapes and transformation operations (e.g., AugMix) by different colors. The straight lines are fit with robust linear regression [41]. We consistently observe high correlation results: Pearson’s correlation ( $|r| > 0.95$ ), Spearman’s correlation ( $|\rho| > 0.93$ ) and weighted Kendall’s correlation ( $|\tau_w| > 0.84$ ). This suggests that BoP + JS is predictive of the suitability of a training set.

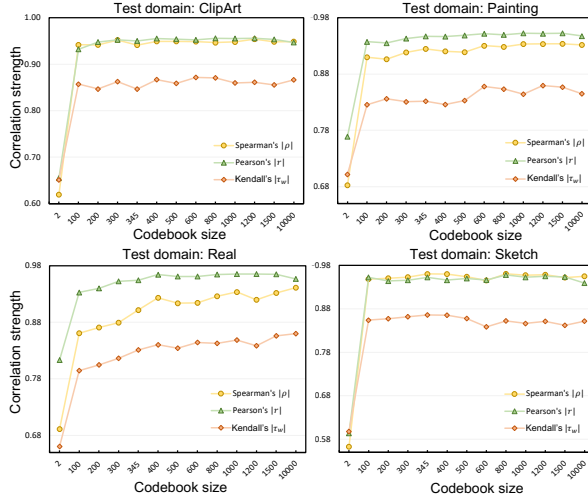


Figure 3. **Impact of codebook size on correlation strength for ResNet-101 on four test domains: ClipArt, Painting, Real and Sketch.** For example, on Real domain, correlation scores  $|\rho|$ ,  $|r|$  and  $|\tau_w|$  are relatively low under a small size and remain stably high when the size is greater than 400.

formance BoP + JS is overall consistent.

**Correlation study with a different model architecture.** We additionally validate the robustness of BoP for ResNet-34 with codebook size 1000. As shown in Table 2, we compare the average correlation scores of BoP + JS, FD, MMD and KID. We see that BoP + JS has consistent performance on two models and remains preferable to characterize training suitability.

## 5. Assessing Test Set Difficulty without Labels

In the task of test set difficulty assessment, we are provided with a labeled training set and a set of unlabeled datasets for testing. Given a classifier trained on the training set, the goal is to estimate the model accuracy on these

test sets without any data annotations. In this section, we first show dataset distance measured by BoP + JS exhibits strong negative correlation with classifier accuracy. We then demonstrate an accuracy predictor based on the BoP representation gives accurate performance estimates compared to state-of-the-art methods.

### 5.1. Experimental Settings

**Correlation study under CIFAR-10 setup.** We conduct a correlation study by comparing BoP + JS with classifier accuracy. Following the same setup in [21], we use a series of datasets sharing the same label space (but usually with distribution shift) with CIFAR-10 [49]. Specifically, we train ResNet-44 classifier [35] on the training set of CIFAR-10, which consists of 50,000 images from 10 classes. Here, we use the CIFAR-10-C benchmark [37] for correlation study, which contains different types of corruptions with 5 levels of severity including per-pixel noise, blurring, synthetic weather effects, and digital transforms. Then, for each dataset, we compute its BoP vector, its BoP + JS from CIFAR-10 training set and the classifier accuracy. In addition to ResNet-44, we also study the RepVGG-A1 [22], VGG-16-BN [72] and MobileNet-V2 [70].

**Predicting classification accuracy under CIFAR-10 setup.** We train a regressor that takes as input the BoP representation and outputs classification accuracy. The regressor is a neural network with 3 fully connected layers and trained on CIFAR-10-C (regression training set). We evaluate accuracy prediction on CIFAR-10.1 [69], CIFAR-10.2 [69] and CIFAR-10.2- $\bar{C}$  [58]. The former two are real-world datasets with natural shift, while the latter one is manually corrupted by the same synthetic shift as [58]. Specifically, we add 10 types of unseen and unique corruptions such as warps, blurs, color distortions and noise additions, with 5 severity levels to CIFAR-10.2. Note that, these corruptions have no overlap with those in CIFAR-10-C [58].

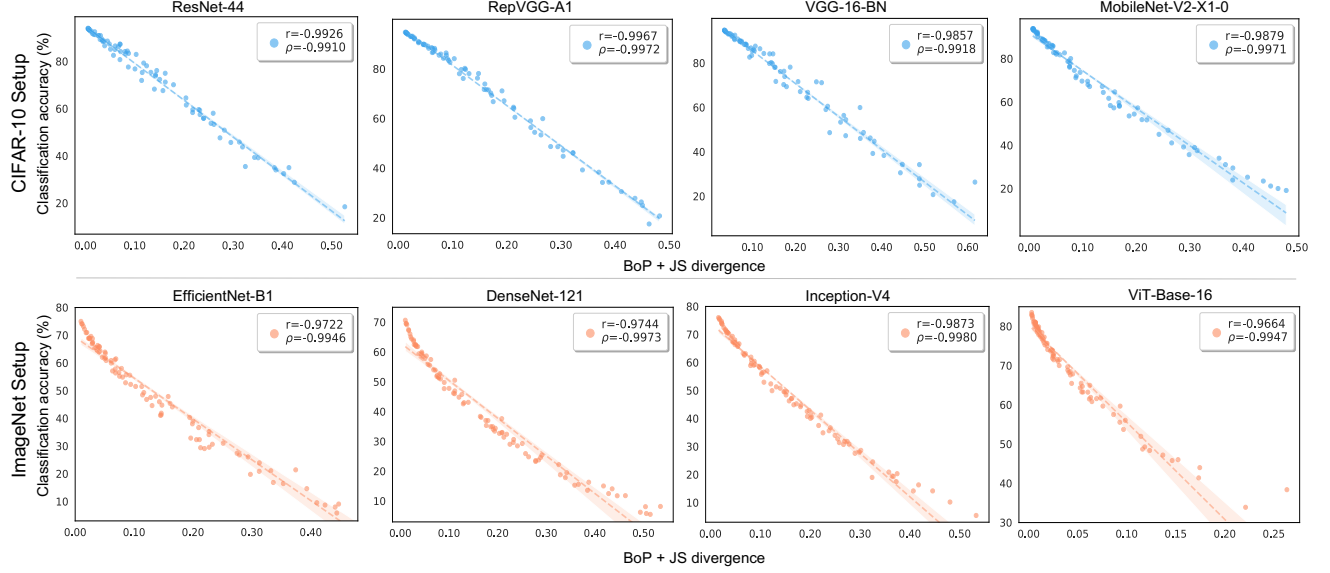


Figure 4. **Correlation between train-test distance measured by BoP + JS and model accuracy.** **Top:** Correlation study under CIFAR-10 setup using ResNet-44, RepVGG-A1, VGG-16-BN and MobileNet-V2. Each data point denotes a dataset from CIFAR-10-C. **Bottom:** Correlation study under ImageNet setup using EfficientNet-B1, DenseNet-121, Inception-V4 and ViT-Base-16. ImageNet-C datasets are used as test sets. The straight lines are fit with robust linear regression [41]. Under both setups, we observe the strong Spearman’s rank correlation ( $|\rho| > 0.98$ ) between BoP + JS and model accuracy.

For the above, we extract image features (output of penultimate layer of ResNet-44) from CIFAR-10 training set. We construct a codebook by dividing the features into 80 clusters with k-means.

**Correlation study under ImageNet setup.** We use DenseNet-121 [40] classifier trained on ImageNet training set. We employ a series of datasets from the ImageNet-C benchmark [36] where the classifier is tested. ImageNet-C uses the same types of corruptions as CIFAR-10-C. We construct a codebook of size 1000 on the ImageNet training set from which images features are extracted by the penultimate layer of DenseNet-121. We project each dataset in ImageNet-C onto the codebook and obtain their BoP representations. When exhibiting linear correlations, we calculate BoP + JS between each ImageNet-C dataset and the training set, and compute classification accuracy. We also use EfficientNet-B1 [78], Inception-V4 [77] and ViT-Base-16 [23] to repeat above procedure for correlation study.

**Evaluation metric.** Same as Section 4.1, we use Pearson’s correlation  $r$  and Spearman’s rank correlation  $\rho$  to show linearity and monotonicity between BoP based dataset distance and model accuracy, respectively. To evaluate the effectiveness of accuracy estimation, we use root mean squared error (RMSE) by calculating the difference between estimated accuracy and ground truth before taking the mean across all the test sets. A larger RMSE means a less accurate prediction, and vice versa.

**Compared methods.** We compare our system with four existing ones. 1) *Prediction score*: it estimates model accuracy using the maximum of Softmax output (*i.e.*, confidence

score). An image with a confidence score greater than a predefined threshold  $\tau \in [0, 1]$  is considered correctly predicted. We select two thresholds ( $\tau = 0.8$  and  $0.9$ ). 2) *Difference of confidence (DoC)* [34] trains a linear regressor mapping average confidence to classifier accuracy; 3) *Average thresholded confidence with maximum confidence score function (ATC-MC)* [31] calculates a threshold on CIFAR-10 validation set and regards an image with a confidence score higher than the threshold as correctly classified; 4) *Network regression ( $\mu + \sigma + FD$ )* [21] trains a neural network that takes as input the feature mean, covariance and Fréchet distance between a set of interest and training set and outputs model accuracy. All methods, if applicable, are compared under the same conditions as our system, *e.g.*, classification training set and regression training set.

## 5.2. Evaluation

**Strong correlation: A test set is difficult (low accuracy) if it is dissimilar to the training set using BoP + JS.** Fig. 4 presents the correlation study of two setups and various classifiers. We observe a very high Spearman’s rank correlation ( $|\rho| > 0.99$ ) in all the scenarios. It indicates that classification accuracy is highly correlated with JS divergence between BoPs of training and test sets. That is, test accuracy drops proportionally to the distance between the given training set and a test set. The results demonstrate BoP + JS between training and test sets is an effective indicator of classification accuracy. More studies are presented in the supplementary materials.

**Effectiveness of the BoP representation in predict-**

Table 3. Method comparison in predicting classifier accuracy under CIFAR-10 setup. We compare four methods: predicted score-based method with hard threshold  $\tau$ , neural network regression based on feature statistics ( $\mu + \sigma + FD$ ) [20], average thresholded confidence with maximum confidence score function (ATC-MC) [30] and difference of confidences (DoC) [34]. We use CIFAR-10.1 and CIFAR-10.2 (both real-world) and CIFAR-10.2- $\bar{C}$  (manually corrupted) as unseen test sets for accuracy prediction. We use RMSE (%) to indicate precision of estimates. In each column, we compare our method with the best of the competing ones. We report results by average of five runs.

Method	CIFAR-10.1	CIFAR-10.2	CIFAR-10.2- $\bar{C}$ (50)					
			Severity 1	Severity 2	Severity 3	Severity 4	Severity 5	Overall
Prediction score ( $\tau = 0.8$ )	4.899	4.800	10.127	12.869	16.809	21.427	24.371	17.910
Prediction score ( $\tau = 0.9$ )	0.297	0.550	3.638	5.078	8.048	11.804	14.108	9.404
ATC-MC [30]	2.650	2.672	3.080	4.306	7.108	11.015	13.040	8.601
DoC [34]	0.490	0.263	<b>2.247</b>	2.916	5.117	9.012	6.637	5.745
$\mu + \sigma + FD$ [21]	0.455	0.561	5.875	5.823	4.724	4.908	6.486	5.602
BoP ( $K = 80$ )	0.218	<b>0.122</b>	2.458	2.818	3.730	5.836	6.451	4.551
BoP ( $K = 100$ )	<b>0.186</b>	0.124	2.849	<b>2.808</b>	<b>3.548</b>	<b>4.025</b>	<b>4.777</b>	<b>3.677</b>

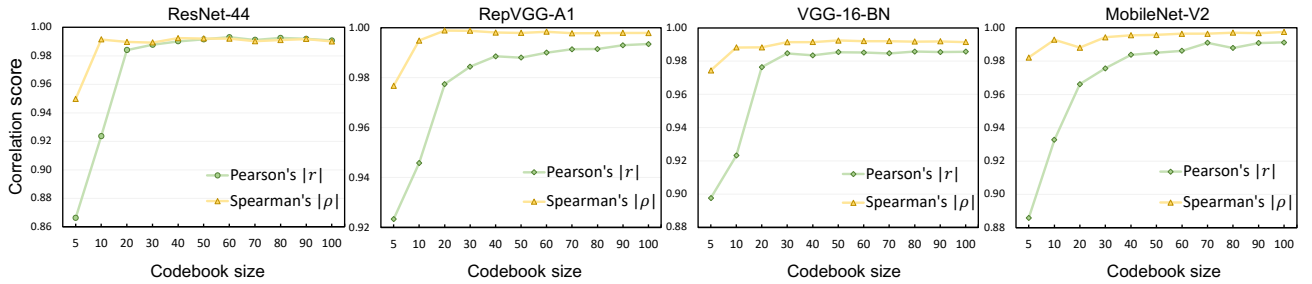


Figure 5. **Impact of codebook size on correlation strength on CIFAR-10-C.** Correlation scores  $|\rho|$  and  $|r|$  are relatively low under a small size and become stably high when the size is greater than 20 for all four model architectures.

### ing classification accuracy on variou unseen test sets.

After performing correlation study, we train a neural network regressor on CIFAR-10-C and test it on a series of test sets. Results are summarized in Table 3. We have the following observations. **First and foremost**, BoP representation achieves the best accuracy prediction performance, evidenced by the lowest RMSE across all the four test scenarios. For example, on the test sets of CIFAR-10.2- $\bar{C}$ , the RMSE of our method is 4.551, which is 1.051 lower than the second best method [21]. This clearly validates the effectiveness of the BoP representation. **Second**, we observe that the “Prediction score” method is unstable. While it has good results under  $\tau = 0.9$  on CIFAR-10.1 and CIFAR-10.2 datasets, it is generally inferior to the competing methods in other test scenarios. Our observation is similar to [21], suggesting that a more robust threshold selection method is needed for this method. **Third**, although BoP has slightly higher RMSE than DoC on Severity 1 of CIFAR-10.2- $\bar{C}$  (2.458 v.s., 2.247), we stress that BoP is overall more stable and effective on real world datasets and other severity levels of synthetic datasets.

**Impact of codebook size** is summarized in Fig. 5 under CIFAR-10 setup. We conduct the study using different sizes on four classifiers. We observe correlation scores first in-

crease and then become stable when codebook size is larger than 20. These results are considered validation and help us use competitive and stable codebook sizes in Table 3.

## 6. Conclusion

This work introduces a *bag-of-prototypes* (BoP) dataset representation to vectorize visual datasets. It first computes a codebook composed of clustering prototypes and then a prototype histogram for a dataset. The BoP vector considers the underlying local semantic distribution of a dataset and is thus more discriminative than global dataset statistics. Specifically, when used in conjunction with JS divergence, the proposed descriptor better captures the underlying relationship across datasets. This advantage is validated by its promising results in two dataset-level tasks: assessing training set suitability and test set difficulty. This work establishes the baseline usage of the BoP scheme, and more investigations and applications will be made in future work.

## Acknowledgements

We thank all anonymous reviewers for their constructive comments in improving this paper. This work was supported by the ARC Discovery Project (DP210102801).



## References

- [1] Alessandro Achille, Michael Lam, Rahul Tewari, Avinash Ravichandran, Subhansu Maji, Charles C Fowlkes, Stefano Soatto, and Pietro Perona. Task2vec: Task embedding for meta-learning. In *Proceedings of the IEEE/CVF International Conference on Computer Vision*, pages 6430–6439, 2019. 1, 2, 5
- [2] David Acuna, Guojun Zhang, Marc T Law, and Sanja Fidler. f-domain adversarial learning: Theory and algorithms. In *International Conference on Machine Learning*, pages 66–75, 2021. 2
- [3] Andrea Agostinelli, Michal Pándy, Jasper Uijlings, Thomas Mensink, and Vittorio Ferrari. How stable are transferability metrics evaluations? In *European Conference on Computer Vision*, pages 303–321. Springer, 2022. 4
- [4] Andrea Agostinelli, Jasper Uijlings, Thomas Mensink, and Vittorio Ferrari. Transferability metrics for selecting source model ensembles. In *Proceedings of the IEEE/CVF Conference on Computer Vision and Pattern Recognition*, pages 7936–7946, 2022. 4
- [5] David Alvarez-Melis and Nicolo Fusi. Geometric dataset distances via optimal transport. In *Advances in Neural Information Processing Systems*, pages 21428–21439, 2020. 2
- [6] Lora Aroyo, Matthew Lease, Praveen Paritosh, and Mike Schaekermann. Data excellence for ai: why should you care? *Interactions*, 29(2):66–69, 2022. 1, 2
- [7] Robert Baldock, Hartmut Maennel, and Behnam Neyshabur. Deep learning through the lens of example difficulty. *Advances in Neural Information Processing Systems*, 34:10876–10889, 2021. 2
- [8] Herbert Bay, Tinne Tuytelaars, and Luc Van Gool. Surf: Speeded up robust features. In *European Conference on Computer Vision*, pages 404–417. Springer, 2006. 3
- [9] Shai Ben-David, John Blitzer, Koby Crammer, Alex Kulesza, Fernando Pereira, and Jennifer Vaughan. A theory of learning from different domains. *Machine Learning*, 79:151–175, 2010. 2
- [10] Shai Ben-David, John Blitzer, Koby Crammer, and Fernando Pereira. Analysis of representations for domain adaptation. In *Advances in Neural Information Processing Systems*, pages 137–144, 2006. 2
- [11] Mikołaj Bińkowski, Danica J Sutherland, Michael Arbel, and Arthur Gretton. Demystifying mmd gans. *arXiv preprint arXiv:1801.01401*, 2018. 4, 5
- [12] Barry Boots, Kokichi Sugihara, Sung Nok Chiu, and Atsuyuki Okabe. Spatial tessellations: concepts and applications of voronoi diagrams. 2009. 4
- [13] Jiefeng Chen, Frederick Liu, Besim Avci, Xi Wu, Yingyu Liang, and Somesh Jha. Detecting errors and estimating accuracy on unlabeled data with self-training ensembles. In *Advances in Neural Information Processing Systems*, 2021. 2
- [14] Gabriella Csurka, Christopher Dance, Lixin Fan, Jutta Willamowski, and Cédric Bray. Visual categorization with bags of keypoints. In *Workshop on statistical learning in computer vision, ECCV*, volume 1, pages 1–2, 2004. 3, 5
- [15] Ekin D Cubuk, Barret Zoph, Dandelion Mane, Vijay Vasudevan, and Quoc V Le. Autoaugment: Learning augmentation policies from data. In *Proceedings of the IEEE Conference on Computer Vision and Pattern Recognition*, 2019. 5, 14
- [16] Ido Dagan, Lillian Lee, and Fernando Pereira. Similarity-based methods for word sense disambiguation. In *Proceedings of the 35th Annual Meeting of the Association for Computational Linguistics and Eighth Conference of the European Chapter of the Association for Computational Linguistics*, pages 56–63, 1997. 3
- [17] Julie Delon and Agnes Desolneux. A wasserstein-type distance in the space of gaussian mixture models. *SIAM Journal on Imaging Sciences*, 13(2):936–970, 2020. 2
- [18] Jia Deng, Wei Dong, Richard Socher, Li-Jia Li, Kai Li, and Li Fei-Fei. Imagenet: A large-scale hierarchical image database. In *Proceedings of the IEEE Conference on Computer Vision and Pattern Recognition*, pages 248–255, 2009. 1, 5, 13
- [19] Weijian Deng, Stephen Gould, and Liang Zheng. What does rotation prediction tell us about classifier accuracy under varying testing environments? In *International Conference on Machine Learning*, 2021. 2
- [20] Weijian Deng and Liang Zheng. Are labels always necessary for classifier accuracy evaluation? In *Proceedings of the IEEE/CVF Conference on Computer Vision and Pattern Recognition*, pages 15069–15078, 2021. 1, 2, 8
- [21] Weijian Deng and Liang Zheng. Are labels always necessary for classifier accuracy evaluation. *IEEE Transactions on Pattern Analysis and Machine Intelligence*, pages 1–1, 2021. 6, 7, 8, 13, 15
- [22] Xiaohan Ding, Xiangyu Zhang, Ningning Ma, Jungong Han, Guiguang Ding, and Jian Sun. Repvgg: Making vgg-style convnets great again. In *Proceedings of the IEEE/CVF Conference on Computer Vision and Pattern Recognition*, pages 13733–13742, 2021. 6
- [23] Alexey Dosovitskiy, Lucas Beyer, Alexander Kolesnikov, Dirk Weissenborn, Xiaohua Zhai, Thomas Unterthiner, Mostafa Dehghani, Matthias Minderer, Georg Heigold, Sylvain Gelly, Jakob Uszkoreit, and Neil Houlsby. An image is worth 16x16 words: Transformers for image recognition at scale. In *Proceedings of the International Conference on Learning Representations*, 2021. 7
- [24] Qiang Du, Vance Faber, and Max Gunzburger. Centroidal voronoi tessellations: Applications and algorithms. *SIAM review*, 41(4):637–676, 1999. 4
- [25] Sabri Eyuboglu, Bojan Karlaš, Christopher Ré, Ce Zhang, and James Zou. dcbench: A benchmark for data-centric ai systems. In *Proceedings of the Sixth Workshop on Data Management for End-To-End Machine Learning*, 2022. 1
- [26] L. Fei-Fei and P. Perona. A bayesian hierarchical model for learning natural scene categories. In *Proceedings of the IEEE Conference on Computer Vision and Pattern Recognition*, pages 524–531, 2005. 3
- [27] Maurice Fréchet. Sur la distance de deux lois de probabilité. *Comptes Rendus Hebdomadaires des Seances de L'Academie des Sciences*, 244(6):689–692, 1957. 2, 4, 5

- [28] David Freedman and Persi Diaconis. On the histogram as a density estimator: L 2 theory. *Zeitschrift für Wahrscheinlichkeitstheorie und verwandte Gebiete*, 57(4):453–476, 1981. 4
- [29] Jianglin Fu, Shikai Li, Yuming Jiang, Kwan-Yee Lin, Chen Qian, Chen Change Loy, Wayne Wu, and Ziwei Liu. Stylegan-human: A data-centric odyssey of human generation. In *European Conference on Computer Vision*, pages 1–19. Springer, 2022. 1
- [30] Saurabh Garg, Sivaraman Balakrishnan, Zachary C Lipton, Behnam Neyshabur, and Hanie Sedghi. Leveraging unlabeled data to predict out-of-distribution performance. In *International Conference on Learning Representations*, 2022. 2, 8, 13, 15
- [31] Saurabh Garg, Sivaraman Balakrishnan, Zachary Chase Lipton, Behnam Neyshabur, and Hanie Sedghi. Leveraging unlabeled data to predict out-of-distribution performance. In *Proceedings of the International Conference on Learning Representations*, 2022. 7
- [32] Amirata Ghorbani and James Zou. Data shapley: Equitable valuation of data for machine learning. In *International Conference on Machine Learning*, pages 2242–2251. PMLR, 2019. 1, 2
- [33] Arthur Gretton, Karsten Borgwardt, Malte Rasch, Bernhard Schölkopf, and Alex Smola. A kernel method for the two-sample-problem. In *Advances in Neural Information Processing Systems*, 2006. 2, 4, 5
- [34] Devin Guillory, Vaishaal Shankar, Sayna Ebrahimi, Trevor Darrell, and Ludwig Schmidt. Predicting with confidence on unseen distributions. In *Proceedings of the IEEE/CVF International Conference on Computer Vision and Pattern Recognition*, pages 1134–1144, 2021. 2, 7, 8, 13, 15
- [35] Kaiming He, Xiangyu Zhang, Shaoqing Ren, and Jian Sun. Deep residual learning for image recognition. In *Proceedings of the IEEE Conference on Computer Vision and Pattern Recognition*, 2016. 5, 6, 13
- [36] Dan Hendrycks and Thomas Dietterich. Benchmarking neural network robustness to common corruptions and perturbations. In *Proceedings of the International Conference on Learning Representations*, 2019. 5, 7, 13
- [37] Dan Hendrycks and Thomas Dietterich. Benchmarking neural network robustness to common corruptions and perturbations. In *Proceedings of the International Conference on Learning Representations*, 2019. 6
- [38] Dan Hendrycks, Norman Mu, Ekin D Cubuk, Barret Zoph, Justin Gilmer, and Balaji Lakshminarayanan. Augmix: A simple data processing method to improve robustness and uncertainty. In *Proceedings of the International Conference on Learning Representations*, 2020. 5
- [39] Martin Heusel, Hubert Ramsauer, Thomas Unterthiner, Bernhard Nessler, and Sepp Hochreiter. Gans trained by a two time-scale update rule converge to a local nash equilibrium. In *Advances in Neural Information Processing Systems*, 2017. 2
- [40] Gao Huang, Zhuang Liu, Laurens Van Der Maaten, and Kilian Q Weinberger. Densely connected convolutional networks. In *Proceedings of the IEEE Conference on Computer Vision and Pattern Recognition*, pages 4700–4708, 2017. 7
- [41] Peter J Huber. Robust statistics. In *International Encyclopedia of Statistical Science*, pages 1248–1251. Springer, 2011. 6, 7, 14, 16
- [42] Hervé Jégou and Ondřej Chum. Negative evidences and co-occurrences in image retrieval: The benefit of pca and whitening. In *European Conference on Computer Vision*, pages 774–787, 2012. 3
- [43] Hervé Jégou, Matthijs Douze, Cordelia Schmid, and Patrick Pérez. Aggregating local descriptors into a compact image representation. In *Proceedings of the IEEE Conference on Computer Vision and Pattern Recognition*, pages 3304–3311, 2010. 3
- [44] Jinguang Jiang, Baixu Chen, Bo Fu, and Mingsheng Long. Transfer-learning-library. <https://github.com/thuml/Transfer-Learning-Library>, 2020. 5, 13
- [45] Ziheng Jiang, Chiyuan Zhang, Kunal Talwar, and Michael C Mozer. Characterizing structural regularities of labeled data in overparameterized models. *arXiv preprint arXiv:2002.03206*, 2020. 2
- [46] Thorsten Joachims. Text categorization with support vector machines: Learning with many relevant features. In *European Conference on Machine Learning*, pages 137–142, 1998. 3
- [47] Thorsten Joachims, Dayne Freitag, Tom Mitchell, et al. Web-watcher: A tour guide for the world wide web. In *International Joint Conference on Artificial Intelligence*, pages 770–777. Citeseer, 1997. 3
- [48] Alexander B. Jung. imgaug. <https://github.com/aleju/imgaug>, 2018. [Online; accessed 30-Oct-2018]. 5
- [49] Alex Krizhevsky and Geoffrey Hinton. Learning multiple layers of features from tiny images. 2009. 4, 6, 13
- [50] David D Lewis and William A Gale. A sequential algorithm for training text classifiers. In *Proceedings of the Seventeenth Annual International ACM-SIGIR Conference on Research and Development in Information Retrieval*, pages 3–12, 1994. 3
- [51] Weixin Liang, Girmaw Abebe Tadesse, Daniel Ho, L Fei-Fei, Matei Zaharia, Ce Zhang, and James Zou. Advances, challenges and opportunities in creating data for trustworthy ai. *Nature Machine Intelligence*, 4(8):669–677, 2022. 1
- [52] Tsung-Yi Lin, Michael Maire, Serge Belongie, James Hays, Pietro Perona, Deva Ramanan, Piotr Dollár, and C Lawrence Zitnick. Microsoft coco: Common objects in context. In *European Conference on Computer Vision*, pages 740–755, 2014. 1
- [53] D.G. Lowe. Object recognition from local scale-invariant features. In *Proceedings of the IEEE International Conference on Computer Vision*, pages 1150–1157, 1999. 3
- [54] James MacQueen et al. Some methods for classification and analysis of multivariate observations. In *Proceedings of the Fifth Berkeley Symposium on Mathematical statistics and probability*, volume 1, pages 281–297. Oakland, CA, USA, 1967. 3
- [55] Christopher Manning and Hinrich Schütze. *Foundations of statistical natural language processing*. MIT press, 1999. 3
- [56] Mark Mazumder, Colby Banbury, Xiaozhe Yao, Bojan Karlaš, William Gaviria Rojas, Sudnya Diamos, Greg Diamos, Lynn He, Douwe Kiela, David Jurado, et al. Dataperf:

- Benchmarks for data-centric ai development. *arXiv preprint arXiv:2207.10062*, 2022. 1, 2
- [57] Andrew McCallum, Kamal Nigam, et al. A comparison of event models for naive bayes text classification. In *AAAI Workshop on Learning for Text Categorization*, pages 41–48, 1998. 3
- [58] Eric Mintun, Alexander Kirillov, and Saining Xie. On interaction between augmentations and corruptions in natural corruption robustness. In *Advances in Neural Information Processing Systems*, 2021. 6, 13
- [59] David Nister and Henrik Stewenius. Scalable recognition with a vocabulary tree. In *Proceedings of the IEEE Conference on Computer Vision and Pattern Recognition*, pages 2161–2168, 2006. 3
- [60] Michal Pándy, Andrea Agostinelli, Jasper Uijlings, Vittorio Ferrari, and Thomas Mensink. Transferability estimation using bhattacharyya class separability. In *Proceedings of the IEEE/CVF Conference on Computer Vision and Pattern Recognition*, pages 9172–9182, 2022. 4
- [61] Amandalynne Paullada, Inioluwa Deborah Raji, Emily Bender, Emily Denton, and Alex Hanna. Data and its (dis)contents: A survey of dataset development and use in machine learning research. *Patterns*, 2021. 1
- [62] Xingchao Peng, Qinxun Bai, Xide Xia, Zijun Huang, Kate Saenko, and Bo Wang. Moment matching for multi-source domain adaptation. In *Proceedings of the IEEE/CVF International Conference on Computer Vision*, pages 1406–1415, 2019. 1, 2, 5, 13
- [63] Xingchao Peng, Yichen Li, and Kate Saenko. Domain2vec: Domain embedding for unsupervised domain adaptation. In *European Conference on Computer Vision*, pages 756–774, 2020. 1, 2
- [64] Florent Perronnin and Christopher Dance. Fisher kernels on visual vocabularies for image categorization. In *Proceedings of the IEEE International Conference on Computer Vision*, pages 1–8, 2007. 3
- [65] Florent Perronnin, Jorge Sánchez, and Thomas Mensink. Improving the fisher kernel for large-scale image classification. In *European Conference on Computer Vision*, pages 143–156, 2010. 3
- [66] James Philbin, Ondrej Chum, Michael Isard, Josef Sivic, and Andrew Zisserman. Object retrieval with large vocabularies and fast spatial matching. In *Proceedings of the IEEE Conference on Computer Vision and Pattern Recognition*, pages 1–8, 2007. 3
- [67] Vladislav Polianskii, Giovanni Luca Marchetti, Alexander Kravberg, Anastasiia Varava, Florian T Pokorny, and Danica Kragic. Voronoi density estimator for high-dimensional data: Computation, compactification and convergence. In *Uncertainty in Artificial Intelligence*, pages 1644–1653. PMLR, 2022. 4
- [68] Anand Rajaraman and Jeffrey David Ullman. *Mining of massive datasets*. Cambridge University Press, 2011. 3
- [69] Benjamin Recht, Rebecca Roelofs, Ludwig Schmidt, and Vaishaal Shankar. Do cifar-10 classifiers generalize to cifar-10? *arXiv preprint arXiv:1806.00451*, 2018. 6, 13
- [70] Mark Sandler, Andrew Howard, Menglong Zhu, Andrey Zhmoginov, and Liang-Chieh Chen. Mobilenetv2: Inverted residuals and linear bottlenecks. In *Proceedings of the IEEE Conference on Computer Vision and Pattern Recognition*, pages 4510–4520, 2018. 6
- [71] Grace S Shieh. A weighted kendall’s tau statistic. *Statistics & Probability Letters*, 39(1):17–24, 1998. 5
- [72] Karen Simonyan and Andrew Zisserman. Very deep convolutional networks for large-scale image recognition. *arXiv preprint arXiv:1409.1556*, 2014. 6
- [73] Sivic and Zisserman. Video google: a text retrieval approach to object matching in videos. In *Proceedings of the IEEE International Conference on Computer Vision*, pages 1470–1477, 2003. 3
- [74] Baochen Sun, Jiashi Feng, and Kate Saenko. Return of frustratingly easy domain adaptation. In *Proceedings of the AAAI Conference on Artificial Intelligence*, 2016. 1, 2
- [75] Baochen Sun and Kate Saenko. Deep coral: Correlation alignment for deep domain adaptation. In *European Conference on Computer Vision*, pages 443–450, 2016. 1, 2
- [76] Swabha Swayamdipta, Roy Schwartz, Nicholas Lourie, Yizhong Wang, Hannaneh Hajishirzi, Noah A Smith, and Yejin Choi. Dataset cartography: Mapping and diagnosing datasets with training dynamics. *arXiv preprint arXiv:2009.10795*, 2020. 2
- [77] Christian Szegedy, Sergey Ioffe, Vincent Vanhoucke, and Alexander A Alemi. Inception-v4, inception-resnet and the impact of residual connections on learning. In *Thirty-first AAAI Conference on Artificial Intelligence*, 2017. 7
- [78] Mingxing Tan and Quoc Le. Efficientnet: Rethinking model scaling for convolutional neural networks. In *International Conference on Machine Learning*, pages 6105–6114, 2019. 7
- [79] Yang Tan, Yang Li, and Shao-Lun Huang. Otce: A transferability metric for cross-domain cross-task representations. In *Proceedings of the IEEE/CVF Conference on Computer Vision and Pattern Recognition*, pages 15779–15788, 2021. 2
- [80] Mariya Toneva, Alessandro Sordoni, Remi Tachet des Combes, Adam Trischler, Yoshua Bengio, and Geoffrey J Gordon. An empirical study of example forgetting during deep neural network learning. *arXiv preprint arXiv:1812.05159*, 2018. 2
- [81] Eric Tzeng, Judy Hoffman, Ning Zhang, Kate Saenko, and Trevor Darrell. Deep domain confusion: Maximizing for domain invariance. *arXiv preprint arXiv:1412.3474*, 2014. 2
- [82] Joaquin Vanschoren. Meta-learning: A survey. *arXiv preprint arXiv:1810.03548*, 2018. 1, 2
- [83] Sebastiano Vigna. A weighted correlation index for rankings with ties. In *Proceedings of International Conference on World Wide Web*, pages 1166–1176, 2015. 5
- [84] Ross Wightman. Pytorch image models. <https://github.com/rwightman/pytorch-image-models>, 2019. 13
- [85] Wei Ying, Yu Zhang, Junzhou Huang, and Qiang Yang. Transfer learning via learning to transfer. In *International Conference on Machine Learning*, pages 5085–5094. PMLR, 2018. 2
- [86] Yuchen Zhang, Tianle Liu, Mingsheng Long, and Michael Jordan. Bridging theory and algorithm for domain adap-

- tation. In *International Conference on Machine Learning*, pages 7404–7413, 2019. [2](#)
- [87] Liang Zheng, Yi Yang, and Qi Tian. Sift meets cnn: A decade survey of instance retrieval. *IEEE Transactions on Pattern Analysis and Machine Intelligence*, 40(5):1224–1244, 2017. [3](#), [5](#)
- [88] Yujie Zhong, Relja Arandjelović, and Andrew Zisserman. Ghostvlad for set-based face recognition. In *Computer Vision–ACCV 2018: 14th Asian Conference on Computer Vision, Perth, Australia, December 2–6, 2018, Revised Selected Papers, Part II 14*, pages 35–50. Springer, 2019. [2](#)



## A. Supplementary

In this supplementary material, we first introduce the experimental details including the training schemes, datasets and computation resources. Then, we show the full results of the correlation study on the task: training set suitability in Fig. 6 and impact of codebook size in Fig. 7. Last, we report the accuracy estimation results on each severity level of CIFAR-10.1- $\bar{C}$  in Table 4 and results on datasets with natural distribution shifts in Fig. 8. After that, we present a correlation study of average thresholded confidence, average confidence, and difference of confidence on ImageNet and CIFAR-10 setups.

### A.1. Experimental Setup

#### A.1.1 Datasets

We carefully check the licenses of all datasets used in the experiment and list the open sources to them.

**DomainNet** [62] (<http://ai.bu.edu/M3SDA/>);  
**ImageNet** [18] (<https://www.image-net.org/>);  
**ImageNet-C** [36] (<https://github.com/hendrycks/robustness>);  
**CIFAR-10** [49] (<https://www.cs.toronto.edu/~kriz/cifar.html>);  
**CIFAR-10-C** [36] (<https://github.com/hendrycks/robustness>);  
**CIFAR-10.1** [69] (<https://github.com/modestyachts/CIFAR-10.1>);  
**CIFAR-10.2** [69] (<https://github.com/modestyachts/CIFAR-10.1>);  
**CIFAR-10- $\bar{C}$**  [58] (<https://github.com/facebookresearch/augmentation-corruption>) We use the corruption method provided in this link to create CIFAR-10.1- $\bar{C}$  and CIFAR-10.2- $\bar{C}$ ;

#### A.1.2 Experiment: Datasets Training Suitability

Follow the same training scheme as [44], we use ResNet-101 [35] architecture pre-trained on ImageNet [18]. The training epoch is 20, the batch size is 32 and the number of iterations per epoch is 2500. The optimizer is SGD with learning rate  $1 \times 10^{-2}$  and weight decay  $5 \times 10^{-4}$ .

#### A.1.3 Experiment: Datasets Testing Difficulty

**CIFAR-10 setup.** We use ResNet-44, RepVGG-A1, VGG-16-BN and MobileNet-V2 classifiers and their trained weights are publicly released by <https://github.com/chenyaofu/pytorch-cifar-models>.

**ImageNet setup.** We use EfficientNet-B1, DenseNet-121, Inception-V4 and ViT-Base-16 classifiers for correlation study. The pretrained models are provided by PyTorch Image Models (timm) [84].

#### A.1.4 Computation Resources

PyTorch version is 1.10.2+cu102 and timm version is 1.5. All experiments run on one 2080Ti and the CPU AMD Ryzen Threadripper 2950X 16-Core Processor.

### A.2. Results of Datasets Training Suitability

#### Full results of correlation study on six test domains.

We present a correlation study of BoP + JS divergence, Fréchet distance, maximum mean discrepancy and kernel inception distance. We use ResNet-101 as the feature extractor. The codebook size for BoP is 1000. All methods use the same feature. Based on their formulae, we use mean and covariance feature to compute them. On all domains, we see that BoP has consistent and superior performance.

**Impact of codebook size on correlation strength for ResNet-101.** In Fig. 7, we find that BoP + JS divergence gives a relatively low correlation and converges to a high correlation when codebook size becomes larger.

**Use Hellinger and Chi-squared to measure the distance between BoP representations.** We test other distances than JS, such as Hellinger and Chi-squared under DomainNet setup with ResNet-101 and codebook size 1000. They yield similar results ( $|\rho| = 0.928, 0.927$ ) as JS ( $|\rho| = 0.929$ ). These results further validate the usefulness of BoP.

**Use ResNet-34 for model accuracy and ResNet-101 to extract features.** We use the extracted features to construct a codebook size 1000 and JS divergence to measure distances. BoP + JS divergence gives  $|\rho| = 0.927$ , and FD, MMD and KID gives  $|\rho| = 0.909, 0.825, 0.899$ , respectively. For Pearson’s correlation, BoP + JS is still the highest ( $|\rho| = 0.959$ ) compared to FD, MMD and KID ( $|\rho| = 0.898, 0.823, 0.864$ ).

### A.3. Results of Datasets Testing Difficulty

**Full results of correlation study on CIFAR-10.1- $\bar{C}$**  is shown Fig. 6. We see that BoP + JS divergence consistently well correlates with classification accuracy on six test domains: ClipArt, Painting, Real, Sketch, Quickdraw, Infograph with  $|r| > 0.95$ ,  $|\rho| > 0.88$  and  $|\tau_w| > 0.81$ .

**The correlation study of BoP + JS, ATC, DoC and AC under CIFAR-10 and ImageNet setups for ResNet-44 and ViT-Base-16, respectively.** We include results of (1) Prediction score ( $\tau = 0.8, \tau = 0.9$ ), (2) Difference of confidence (DoC) [34], (3) Average thresholded confidence with maximum confidence (ATC-MC) [30], Network regression ( $\mu + \sigma + FD$ ) [21] and BoP with codebook size 80 or 100 on CIFAR-10.1- $\bar{C}$  in Table 4. We see that BoP is overall more predictive of model testing difficulty compared with other methods. We also present the correlation study of BoP + JS, ATC-MC, DoC and average confidence (AC) under CIFAR-10 setup and ImageNet setup in Fig. 9.

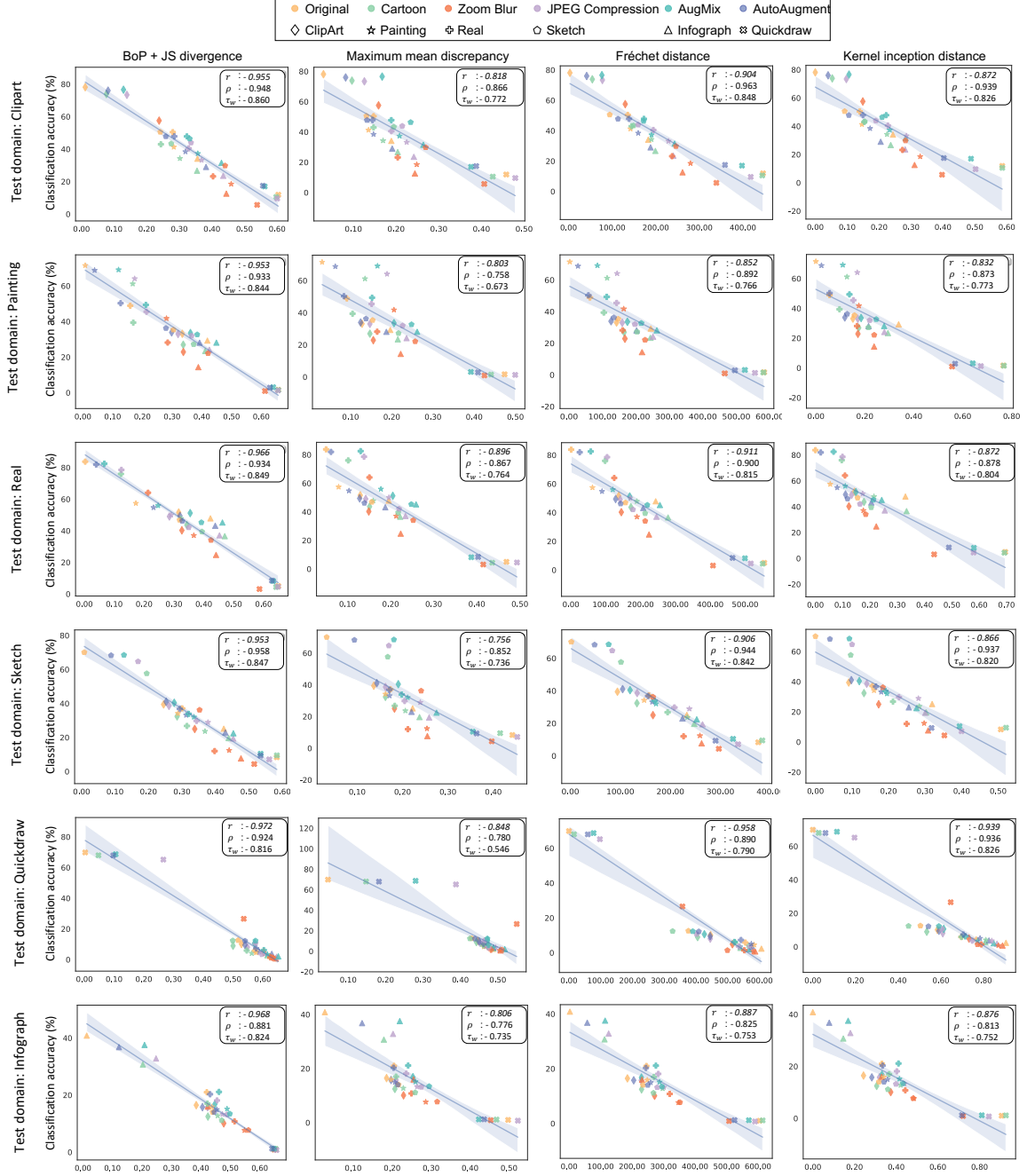


Figure 6. **The full results of comparing training suitability of datasets.** Each point denotes a model. The models trained on transformed training sets are marked with shapes and each shape denote one specific transformation operation (e.g., AutoAugment [15]). The straight lines are fit with robust linear regression [41].

**Results on datasets with natural distribution shifts for Inception-V4.** In addition to datasets with synthetic shifts (*i.e.* ImageNet-C), we explore the effectiveness of BoP on datasets with natural shifts. Under ImageNet setup, we include results of ImageNet-V2-A/B/C and ImageNet-Sketch for Inception-V4. From Fig. 8, we observe that four

datasets (red dots) still lie on the trend of ImageNet-C (grey dots). This means that BoP still effectively captures the distributional shift of four real-world datasets.

**DomainNet setup for test set difficulty.** We also use 36 domains from DomainNet setup for datasets testing difficulty. We use ResNet-101 trained on ‘Real’ domain to

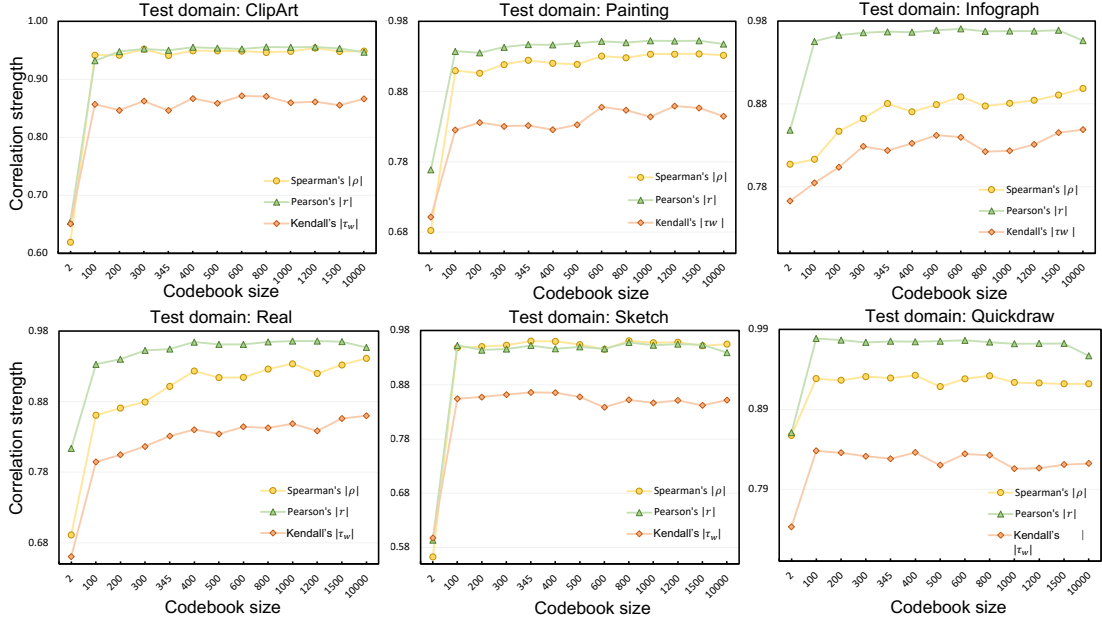


Figure 7. **The impact of codebook size on correlation strength on six test domains: ClipArt, Painting, Infograph, Real, Sketch and Quickdraw.** We observe on six domains that BoP+JS gives low correlation with a small codebook and maintains stably high when codebook size becomes larger.

Method	CIFAR-10.1- $\tilde{C}$					
	L1	L2	L3	L4	L5	Overall
$\tau = 0.8$	10.43	13.02	16.44	21.35	24.44	17.90
$\tau = 0.9$	4.00	5.26	8.36	11.90	13.98	9.49
ATC-MC [30]	3.47	4.63	7.64	11.15	12.85	8.73
DoC [34]	2.48	2.90	6.30	8.80	6.87	5.98
$\mu + \sigma + FD$ [21]	6.46	6.12	5.51	4.58	5.52	5.67
BoP ( $K = 80$ )	1.89	2.34	3.56	5.92	6.32	4.40
BoP ( $K = 100$ )	2.14	2.83	3.98	3.68	5.52	3.81

Table 4. Method comparison in predicting classifier accuracy under CIFAR-10 setup. We report RMSE (%) on each severity level of CIFAR-10.1- $\tilde{C}$ .

extract features and construct a codebook of size 1000. We conduct a correlation study between BoPs of the rest 35 domains and model accuracy. We compare BoP + JS with ATC, DoC and AC. We find that BoP + JS shows the strongest correlation ( $|r| = 0.959$ ,  $|\rho| = 0.972$ ) while the second best ATC has  $|r| = 0.957$ ,  $|\rho| = 0.924$ .

#### Analysis of the sensitivity of BoP to dataset size.

Datasets in DomainNet also vary widely in size (from 48k to 173k) where BoP works well on both dataset-level applications. We further studied the impact of dataset size on

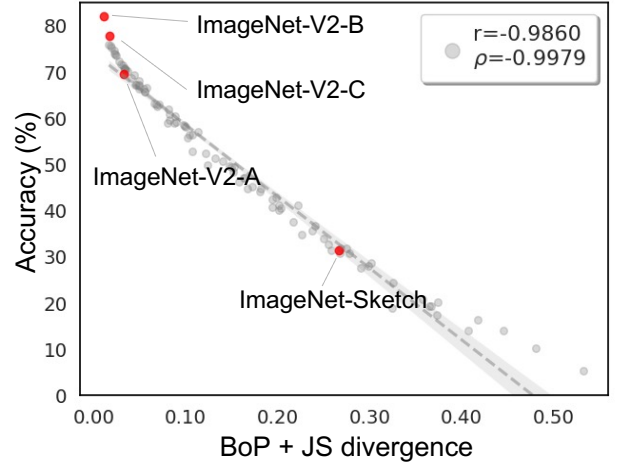


Figure 8. **Results on four datasets with natural shifts for Inception-V4: ImageNet-V2-A/B/C and ImageNet-Sketch.** We find that four new datasets (red dots) still lie on the original trend of ImageNet-C (grey datasets).

DomainNet in dataset testing difficulty by randomly sampling 1% to 10% of data from each test set. Correlation of all methods decreases but BoP remains the best:  $|\rho|$  is 0.909, 0.857, 0.849 (decrease from 0.973, 0.914, 0.925) for BoP, DoC and ATC, respectively.

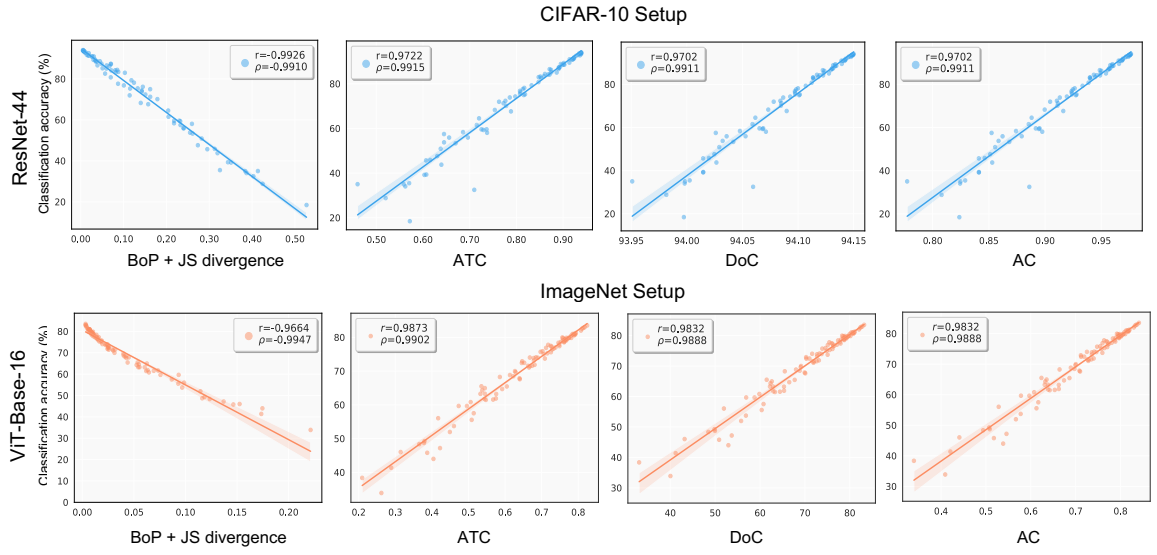


Figure 9. **The correlation study of BoP + JS, ATC, DoC and AC under CIFAR-10 and ImageNet setups.** **Top:** Correlation study under CIFAR-10 setup using ResNet-44. In each figure, a point denotes a dataset from CIFAR-10-C benchmark. **Bottom:** Correlation study under ImageNet setup using ViT-Base-16. In each figure, a point denotes a dataset from ImageNet-C benchmark. The straight lines are fit with robust linear regression [41]. We observe that BoP+JS gives a higher Spearman’s correlation on both setups.